Journal of Social Research

P-ISSN:2827-9832
E-ISSN: 2828-335x
Vol. 5, No. 9, August 2026
http://ijsr.internationaljournallabs.com/index.php/ijsr

Multi-Frequency Source Wavelet Analysis on Pinch-Out Structure Model: The Comparison Between 45 HZ and Broadband Frequency

Dipika Anggun Ardianti*, Terdy Kistofer
Universitas Hasyim Asy'ari, Indonesia
Email: dipikaanggun@unhasy.ac.id*, terdykistofer@unhasy.ac.id

Keywords:
Wedge model;
Broadband frequency;
tuning thickness;
wavelet.

ABSTRACT

Thin-bed and pinch-out structures remain among the most challenging geological features to interpret accurately using conventional seismic reflection methods because wavelet interference alters reflection amplitude, waveform characteristics, and apparent layer thickness. These limitations often reduce vertical resolution and introduce uncertainty in identifying stratigraphic boundaries and estimating reservoir geometry. This study aims to compare the seismic responses generated by a conventional 45 Hz Ricker wavelet and a broadband frequency wavelet in imaging a wedge-shaped pinch-out model, with particular emphasis on waveform characteristics, amplitude behavior, and tuning thickness. The research employed a forward seismic modeling approach by constructing a wedge model with layer thicknesses varying from 50 ms to 1 ms. Reflection coefficients derived from the model were convolved separately with a single-frequency 45 Hz Ricker wavelet and a broadband wavelet synthesized from frequencies ranging from 1 to 150 Hz. The resulting synthetic seismograms were analyzed using waveform comparison, amplitude variation with interface separation, apparent thickness evaluation, and the Rayleigh resolution criterion. The results demonstrate that the 45 Hz wavelet produces a distinct tuning thickness of approximately 9 ms, characterized by maximum constructive interference and pronounced amplitude extrema. In contrast, the broadband wavelet exhibits significantly improved vertical resolution, with only minor tuning effects occurring at approximately 2–1 ms, enabling clearer separation of closely spaced reflectors and a more accurate representation of wedge termination. These findings indicate that broadband frequency wavelets substantially reduce tuning-related ambiguity and provide superior imaging performance for thin-bed interpretation, thereby supporting more reliable seismic stratigraphic analysis and reservoir characterization.

INTRODUCTION

Seismic responses observed in processed seismic sections may lead to ambiguous interpretations because existing thin layers may not be recognizable by interpreters (Alcalde and Bond, 2022; Gunderson *et al.*, 2022; An and Dong, 2023; Anna *et al.*, 2026). Amplitude variations and waveform characteristics are commonly used to identify geological boundaries (Schwardt *et al.*, 2022; Verma *et al.*, 2022; Ren *et al.*, 2026; Zhang *et al.*, 2026). However, additional factors should be carefully considered when studying potential changes in waveform, amplitude, and phase information resulting from variations in geological

conditions during sedimentation processes. From a geological perspective, thin layers can be formed through rapid sedimentation processes involving materials with different grain sizes. Wedge-shaped sand layers may indicate transgressive depositional processes characterized by layer thinning (Meissner and Meixner, 1969). Two-layer boundaries with different separations produce corresponding changes in waveform characteristics due to interference between reflected signals. The characteristic waveform and the time interval between reflections may provide information regarding layer thickness (Gochioco, 1991). The relationship among layer thickness, interface separation resolution, signal wavelength, and waveform interference was investigated by Okaya (1995). To validate previous studies on thin-layer detection, this study simulated a wedge model, analyzed waveform behaviour, and varied the source-wavelet frequency to understand the ideal seismic responses associated with geological layers of varying thicknesses.

The implications of limited seismic resolution extend beyond the inability to measure bed thickness (Yang *et al.*, 2023; Chatterjee, Zhao and Zhang, 2025; Chang *et al.*, 2026). Constructive interference may generate anomalously high amplitudes that resemble bright spots, whereas destructive interference may weaken or eliminate reflections associated with actual geological boundaries. Tuning effects can therefore obscure pinch-out terminations, produce misleading structural or stratigraphic interpretations, and complicate the identification of direct hydrocarbon indicators (Khalid *et al.*, 2023; Peploe, 2026). This limitation also affects amplitude-versus-offset (AVO) or amplitude-versus-angle (AVA) interpretation because the measured amplitude of a thin bed represents the combined response of closely spaced interfaces rather than the reflectivity of an individual boundary. Synthetic wedge modelling has demonstrated that amplitudes remain relatively stable when the layer is sufficiently thick, increase when wavelet sidelobes interfere constructively, and subsequently decrease when the principal lobes overlap destructively near the wedge tip. These variations indicate that amplitude anomalies in thin-layer settings must be evaluated in relation to layer thickness, impedance contrast, wavelet shape, dominant frequency, and bandwidth.

Within this broader context, the frequency content of the source wavelet represents a critical variable because it controls the wavelength and temporal duration of the seismic response. A wavelet dominated by a relatively low or narrow frequency range generally exhibits a broader central lobe and longer sidelobes, causing reflections from closely spaced boundaries to overlap at greater layer thicknesses. In contrast, broadband seismic data combine low- and high-frequency components to produce a more compact seismic pulse. Higher frequencies sharpen the central wavelet peak and improve the separation of closely spaced interfaces, whereas lower frequencies reduce sidelobe energy and support more stable impedance interpretation. Consequently, broadband seismic data are generally less affected by severe tuning effects and can provide clearer images of pinch-outs, thin reservoirs, and subtle structural boundaries compared with conventional narrow-band data. However, the extent to which a constructed broadband Ricker wavelet improves the recognition of a progressively thinning wedge relative to a conventional single-frequency wavelet requires controlled investigation because real seismic responses are also influenced by attenuation, noise, nonstationarity, and processing workflows.

Several previous studies have established the theoretical foundation for investigating thin-bed seismic responses. Widess (1973) demonstrated that the composite amplitude and apparent

timing of reflections vary systematically as bed thickness decreases, providing one of the most influential criteria for defining a seismically thin bed. Gochioco subsequently examined tuning effects and interference responses from thin beds and coal seams, demonstrating that waveform and amplitude behaviour could be used to identify the transition from separated reflectors to tuned seismic events. Okaya investigated the spectral properties controlling seismic resolution and emphasized the relationship among signal wavelength, interface separation, frequency content, and the resolving capability of seismic data. Collectively, these studies confirm that seismic resolution is not determined by bed thickness alone but by the interaction between geological geometry and the source wavelet. Nevertheless, much of the classical literature has focused on single dominant-frequency wavelets or simplified theoretical resolution criteria, leaving opportunities for direct comparisons between conventional single-frequency and synthetically constructed broadband responses.

Recent research has extended thin-bed analysis through multiple-frequency decomposition and seismic bandwidth enhancement. Ye et al. (2019) investigated channel-thickness imaging using multiple-frequency components and demonstrated that combining frequency-dependent responses can improve the estimation of relative formation thickness. A spectrum–cepstrum approach has also been proposed to enhance seismic data for delineating thin oil-bearing sandstone layers that cannot be adequately resolved in conventional seismic sections. Kwietniak et al. applied post-stack spectral blueing to thin unconventional formations and reported that the enhanced seismic volume revealed previously indistinguishable horizons and additional anomalous zones while preserving relative amplitude relationships. More recently, Manzoor and colleagues demonstrated that incorporating higher-frequency information could improve thin-bed reservoir characterization and produce seismic results consistent with geological facies information. These findings confirm the value of increasing or reconstructing frequency bandwidth; however, they primarily focus on processing algorithms, field data applications, or reservoir-characterization workflows rather than controlled comparisons of wavelet-dependent tuning behaviour within an idealized pinch-out model.

Despite these contributions, an important research gap remains in the explicit and quantitative comparison between a commonly used single-frequency Ricker wavelet and a broadband wavelet constructed by combining a wide range of Ricker frequency components under identical geological and petrophysical conditions. Previous studies have generally established the theoretical relationship between wavelength and tuning thickness or proposed methods for enhancing seismic resolution. However, fewer studies have simultaneously compared waveform evolution, interface amplitude, apparent thickness, destructive interference, and tuning-thickness position for single-frequency and broadband sources within the same progressively thinning wedge model. This gap is significant because improvements in visual resolution do not automatically explain how amplitude extrema, peak-to-trough separation, and apparent wedge termination vary as functions of frequency bandwidth. Therefore, a controlled synthetic model is required to isolate source-wavelet effects from noise, attenuation, geometrical spreading, multiples, and other complexities encountered in field seismic data.

The present research addresses this gap by modelling a wedge-shaped layer with temporal thickness decreasing from 50 ms to 1 ms. The wedge has a velocity of 1,768 m/s,

whereas the surrounding formation has a velocity of 1,481 m/s, with a constant density of 1 g/cm³ assigned to simplify the analysis of acoustic impedance contrasts. A reflectivity sequence derived from this model is convolved separately with a zero-phase 45 Hz Ricker wavelet and a broadband source wavelet constructed by summing Ricker components from 1 to 150 Hz at 1 Hz intervals. The resulting synthetic seismograms provide a controlled basis for examining reflector separation, waveform interference, amplitude variations at the upper and lower interfaces, and the relationship between true and apparent temporal thickness. Preliminary results from the model indicate that the 45 Hz wavelet produces a distinct tuning thickness at approximately 9 ms, whereas the broadband response exhibits only minor tuning effects at approximately 2 ms and 1 ms. These contrasting responses make the wedge model particularly suitable for demonstrating how frequency content influences seismic detectability and resolution.

The urgency of this research arises from the continued risk of interpreting tuned seismic amplitudes as direct representations of geological thickness or impedance contrasts. In practical seismic interpretation, an apparently continuous high-amplitude event may represent a tuned composite reflection rather than a thick reservoir, while amplitude weakening near a pinch-out may be incorrectly interpreted as a reduction in reservoir quality. Such misinterpretations may affect horizon picking, stratigraphic mapping, volumetric estimation, well placement, and the evaluation of subtle exploration targets. Although advanced deconvolution and bandwidth-extension methods are increasingly applied to enhance seismic resolution, their interpretation still requires a comprehensive understanding of the physical relationship among wavelet frequency, bed thickness, and interference behaviour. Recent physics-assisted and spectral-fitting approaches continue to identify wavelet estimation and high-frequency recovery as central challenges in seismic-resolution enhancement, confirming that fundamental wavelet-controlled modelling remains relevant for validating advanced workflows.

Accordingly, the novelty of this research lies in its integrated comparison of a 45 Hz single-frequency Ricker wavelet and a synthetically generated 1–150 Hz broadband wavelet using identical pinch-out geometry, reflection coefficients, and convolutional assumptions. Rather than evaluating frequency effects solely through visual inspection, this study combines synthetic-section analysis, upper- and lower-interface amplitude curves, apparent-versus-true thickness cross-plots, and Rayleigh-based tuning evaluation. The purpose of this research is to determine how source-wavelet bandwidth influences the seismic expression and resolvability of a progressively thinning wedge. Specifically, the study aims to compare waveform and amplitude variations produced by the two source wavelets, identify their respective tuning thicknesses, and assess their capability to represent the top, base, and termination of the wedge. This research provides a synthetic reference framework for interpreters evaluating thin-bed and pinch-out responses, while its practical contribution lies in supporting more reliable wavelet selection, frequency assessment, horizon interpretation, and recognition of frequency-dependent tuning effects in seismic reservoir characterization.

METHOD

The methods used in this study involved creating a wedge model, generating both single-frequency and broadband source wavelets, performing convolution between the wavelets and the reflection coefficient series, and analyzing the resulting synthetic seismograms.

Wedge Model

We generated the wedge model (Figure 3.1). The wedge model with formation thickness changing from 50 ms to 1 ms in time to mimic seismic stacked section. The wedge shaped formation has velocity of 1768 m/s. The surrounding formation has velocity 1481 m/s. The same density value of 1 g/cc is assumed. The reservoir geometry consists of two kinds of rocks properties. The model tries to define the wedge layer with 50 ms thick and became thinner with the increasing offset distance.

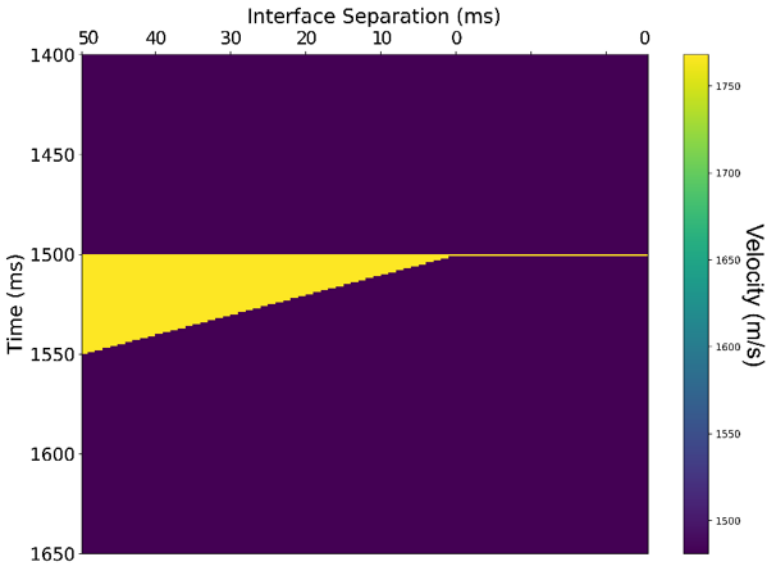

Figure 1. Wedge Model Geometry

Convolutional Model and Wavelet

The convolution process is the cornerstone of the seismic modelling. The idea is to model the real seismic trace through convolving seismic source pulse with a reflection coefficient series. Reflection coefficient is related to acoustic impedance variations which define as the product of velocity and density. The computations follow the standard convolutional approach which is based on the assumptions that a plane wave propagation across boundaries of horizontally homogeneous layers and does not take into account geometrical divergence, non-elastic absorption, wavelet dispersion, transmission losses, wave mode conversions and multiple reflections. These issues should be taken care of in the data pre-conditioning stage (Veeken, 2007). Additional assumption as emphasis by Russell (1988) is that no noise component, the plane waves impinging at normal incidence, the source wavelet w(t) does not change with travel time (stationary). Further assumption as stated by Simm & Bacon (2014) that the source wavelet has zero phase and the reflectivity is a random process. While performing forward simulation, for simplification, we prefer zero phase wavelet which

has symmetrical waveform for ease the interpreter to correlate the interface with the horizon in the seismic section. A zero phase wavelet is ideal for the interpreter because it has a strong dominant central through or peak at zero time, has better resolution, assist user to see the lithological changes, and the seismic waveform commonly will change it shape when the impedance changes. There are a number of idealized wavelet type, however I tend to used Ricker wavelet (eqn. 3.1). The Ricker wavelet is defined by a single central frequency and has two side lobes. It is a zero phase and has a symmetrical waveform shape. It has strong dominant central through or peak at zero time. Ricker wavelets has the period measure from the time interval between the central peak of the waveform to each two side lobes. Simm and Bacon (2014) advised that the Ricker wavelet is useful given its simplicity and often for first pass usage to generate synthetics. However, Hosken (1988) against the use of Ricker wavelets, because real seismic data generally has a flat topped spectral shape as opposed to a peaked amplitude spectrum represented by Ricker wavelet.

$$W(t) = (1 - 2\pi^2 f^2 t^2)\exp(-\pi^2 f^2 t^2). \qquad (2)$$

Where W(t) is the wavelet as a function of time, f is the modeled frequency corresponds to peak amplitude spectrum (Hz), and t is time (s).

Wavelet take an important role to improve interpretability to recognize the top and base of formation layer, we create the synthetic data with two kind of wavelet to evaluate seismic waveform responses, the first wavelet is a single 45 Hz frequency. While for multi-frequency wavelet construction, we also utilize Ricker wavelet equation. The source time function with the broadband frequency was produced in order to imitate the source wavelet of the real seismic data. As described previously that Ricker wavelet is defined by single central frequency, therefore we sequentially summing the Ricker wavelet with frequency 1 until 150 Hz with incremental frequency of 1 Hz. Figure 2 (a.) A broadband frequency wavelet response cover 1 to 150 Hz. (b.) A Ricker wavelet with a single 45 Hz frequency is used to convolve with reflectivity sequence. Figure 3 illustrates the synthetic seismogram response, both single and broadband frequency wavelet was used to convolve with the reflection coefficient of the layer boundaries.

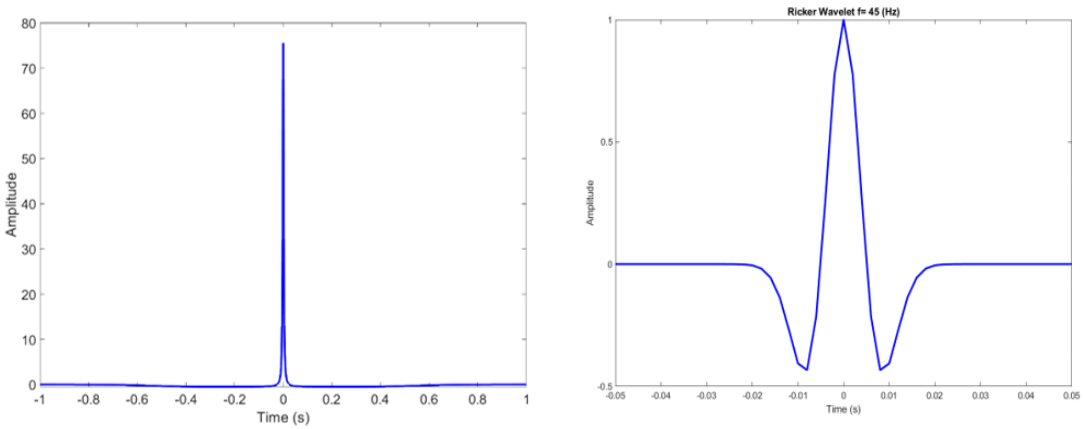

Figure 2. source wavelet (a) Broadband frequency wavelet, (b) 45 Hz frequency wavelet

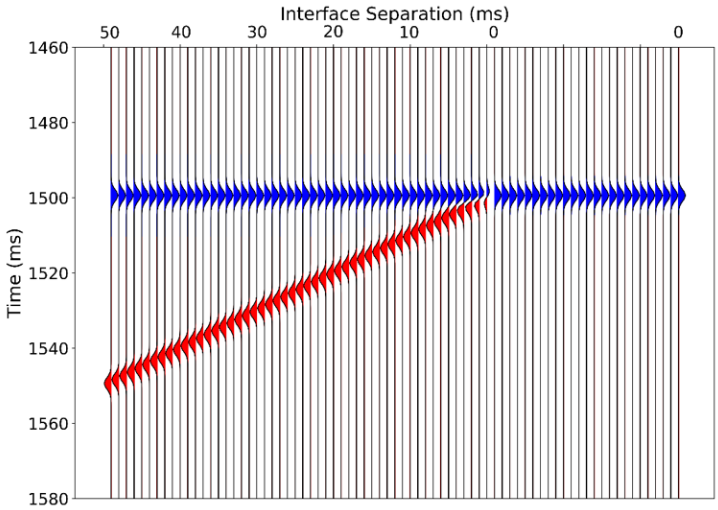

Figure 3. Broadband synthetic section of wedge model

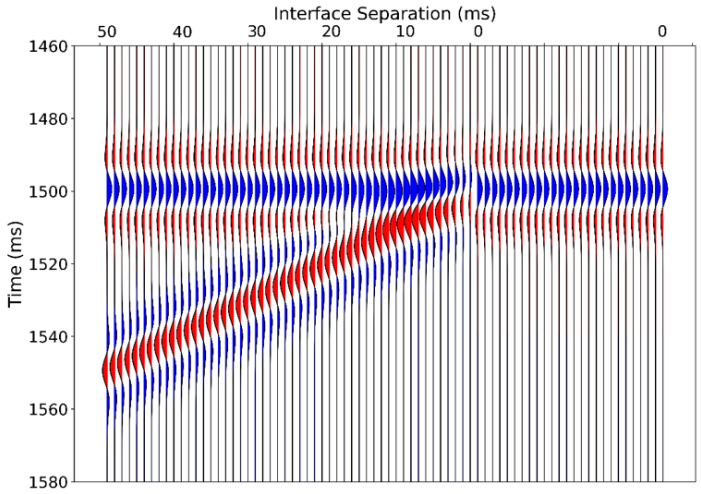

Figure 4. The 45 Hz Ricker source wavelet is used to construct the zero-offset synthetic seismograms for a wedge model

RESULT AND DISCUSSION

The synthetic seismogram as the result of convolution process, shows in figure 3 and figure 4. Figure 3 the synthetic seismogram is constructed using 45 Hz Ricker source wavelet, while figure 3, the synthetic seismogram is generated by broadband frequency source wavelet. Both of them reveal that waveform and amplitude changes. The waveform changes mainly attribute to the interference of reflections caused by the geometry and Interface Separation (IS) of wedge model.

Figure 5 illustrate the amplitude variation with IS. for the top and bottom interfaces of a wedge model generated by a broadband source (1-150 Hz). Figure 5a the corresponding amplitude for upper interface. Figure 5b the AVO response for lower interface. The top interface with peak amplitude and bottom interface with through amplitude value in flat layer

and dipping layer respectively has the same reflection strength with opposite polarity. The constant amplitude occurred between 50-7 ms for both interfaces. The amplitude start to drop (increase) at 6 ms thickness for the top (bottom) interface. The tuning thickness is at the maximum amplitude or at the initiation of constant peak-trough waveform thickness. While, for broadband wavelet, synthetic responses show no obvious amplitude maximum. When the layer get thinner the two reflectors are overlap, and it create the wave interference therefore the amplitude is tuned by the variation of layer's thickness. The amplitude will change when the IS decreases and approaching tuning thickness. Such amplitude variation behavior is related to the interference occurred from the thin layer model. When the thickness becomes zero, complete destructive interference occurred. Wavelet changes its waveforms are strongly associated with the vertical variations of acoustic impedance which produce different level of waveform and phase changes in the recorded reflections. Three factors must considered for each reflection sequence, these are (1) the reflection event time, (2) the additional amplitude scaling by the reflection coefficient and (3) waveform of the wavelet (Hilterman, 2013). The computed responses can be further modified by the wave interference and attenuation such that phase information and impedance difference between the two reflection events could become more complex.

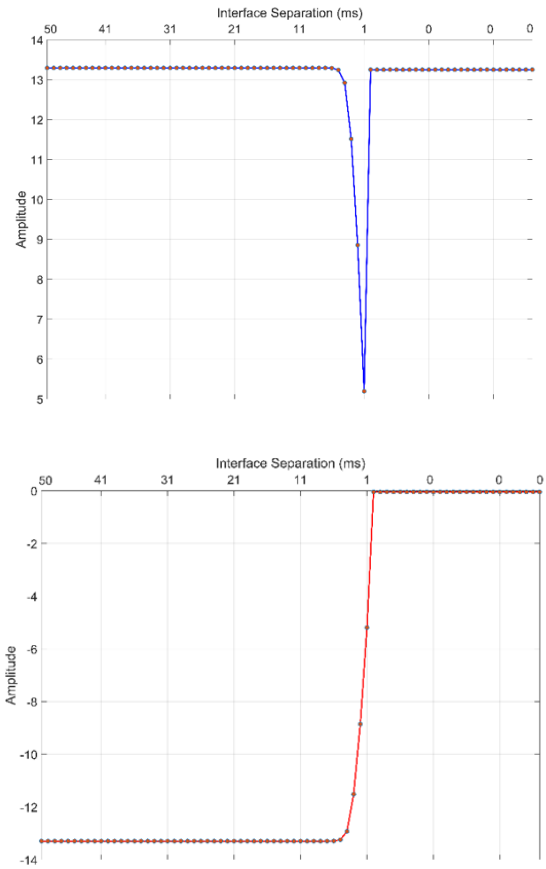

Figure 5. The corresponding amplitude varying with offset (AVO) distance (or interface separation) for (a) the upper layer, and (b) for the bottom interfaces of a wedge model generated by a broadband source (1-150 Hz).

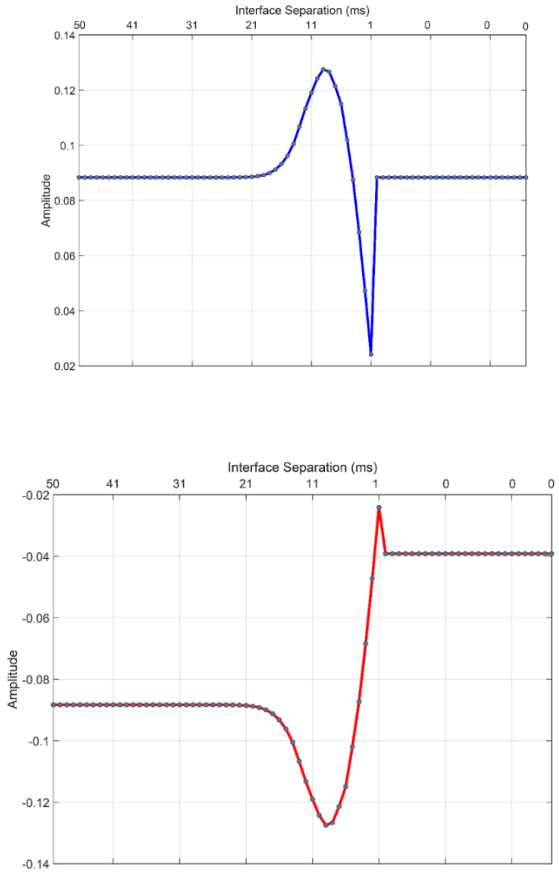

Figure 6. the amplitude curve of source wavelet 45 Hz (a) the upper layer, and (b) for the bottom interfaces.

To better understood and investigate the source-dependent waveform changes, amplitude signature changes associate with tuning effects in the computed synthetic responses, single frequency response should be emphasis. The technique to estimate thin layer response through time and amplitude analyses is referred as TAMP (time and amplitude). Figure 4 shows synthetic seismograms and its corresponding amplitude features generated by convolving a 45 Hz Ricker wavelets with a specified reflectivity in a defined wedge model. Figure 4 shows the computed zerooffset seismograms produced by the wedge model. The synthetic seismogram responses show distinct signal separation at large IS while gradually shows more obvious interference occurred at thinner layer. Note that the variations in waveform, amplitude, apparent time-shift with up dip feature revealed at wedge tip, truncated reflection when IS become 0 ms, the weakening in amplitude before and after tuning effect occurred across the wedge tip are clearly revealed. Figure 6 shows the corresponding amplitude variation with offset or its corresponding IS. For a wedge model with an opposite-sign pair of interfaces, the tuning thickness is at the amplitude extremum (either the "maximum" or "minimum") amplitude (called tuning amplitude). Tuning thickness can be also corresponding to the initiation of constant peak to-trough waveform which also called the two-way apparent thickness (in time unit). The interface separation of 9 ms corresponds to maximum absolute amplitude is the tuning thickness. The amplitude at the bottom interface shows the minimum amplitude occurred at the same IS of 9 ms. For top reflection beyond

wedge tip, amplitude value maintains the same as those amplitudes greater than 21 ms. For bottom reflection, the picked amplitude variation beyond wedge tip corresponds to the side lobe of the reflections at the top interface. The tuning phenomena occurs differently when a source wavelet with different frequency content convolved with the reflectivity.

The AVO curves show in Figure 6 have relatively consistent constant amplitude before 21 ms. For IS less than 21 ms, amplitude gradually increased before reach its maximum. At 9 ms time separation of the two layer interface, tuning effect show maximum for the top interface and minimum for the bottom interface amplitude. After amplitude reach its extreme, amplitude further decreases (top) or increase (bottom). The 9 ms time IS indicates the tuning thickness that can be achieved by 45 Hz wavelet.

A typical detection and resolution to measure and interpret bed thickness is to present the cross plot of the apparent thickness versus two-way true thickness (Fig. 7) for broadband (red) and a single 45 Hz frequency (blue) responses. The two-way peak to trough time difference is the apparent thickness. The thickness used in both axes are in time-separation unit of ms. The corresponding AVO curves which were shown in Figure 6 and figure 5 can be also superimposed on the cross plot. For clarity, only 45 Hz AVO curves for the top and bottom interfaces are shown. The tuning thickness is at the time point where apparent thickness (blue curve) decrease then increase again and return to the point where red and blue curves are crossing to each other at 9 ms. The time-thickness curves between single and broadband data show the tuning thickness as function of source wavelet bandwidth and central frequency. From the two single frequency AVO curves (green and purple) the tuning thickness can be also detected at 9 ms while the broadband response cannot depict obvious tuning effect but show minor tuning thickness feature at 2 and 1 ms IS.

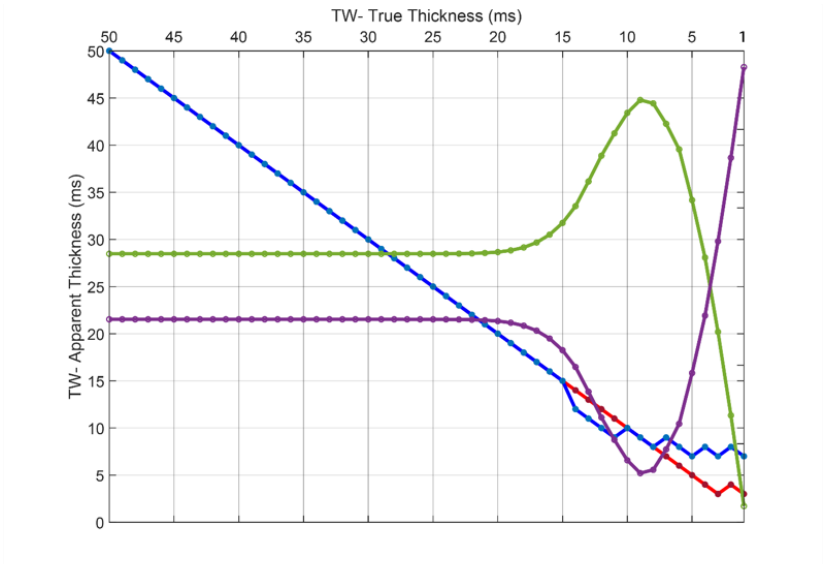

Figure 7. The cross plot of two-way apparent thickness versus two-way true thickness for broadband (red) and a single 45 Hz frequency (blue) responses for the top interface. From single frequency response the tuning thickness can be detected at 9 ms thickness (green and purple curves).

The resolving power of reflections from thin beds in time and frequency can be quantitatively examine its vertical resolution of stacked seismic data once the wavelet is known. The Rayleigh's criteria on the resolution limit is defined by the central-maximum to adjacent-minimum (peak-to-trough) time interval of a band-limited wavelet. The time interval has a finite width which is inversely proportional to aperture width. Rayleigh's limit of resolution occurs when two signals produce a diffraction pattern which are separated by the peak-to-trough time interval. Diffraction patterns thus set an upper limit resolution when two signals interfere with each other. Tuning thickness based on Rayleigh's criterion is defined by the diffraction wavelet width (or trough interval, b) or peak-to-tough time interval (b/2 or first zero-crossing interval). Based on Rayleigh criterion, the tuning thickness occurred at time 9 ms for a 45 Hz Ricker source wavelet.

Different source wavelet with different frequency bandwidth will produce different tuning thickness at different IS location. Table 3.1 shows the extracted tuning thickness from broadband and single frequency responses. Using broadband source wavelet, judging from AVO curve show that the tuning thickness is very close to zero. Such situation indicates our simulation with 1-150 Hz bandwidth Ricker source wavelet will provide sufficient resolution. While for a single 45 Hz source wavelet, the AVO, show that tuning thickness is around 9 ms. Additional information based on time-thickness crossplot for wedge model with opposite impedance and Rayleigh's criterion, the tuning thickness also occurred at time 9 ms. The tuning thickness is the point where the two-way apparent thickness (peak-to-trough time) is precisely equal to the true thickness (spike separation).

Table 1. Identification Tuning Thickness of wedge model

	Rayleigh's Criterion
Broadband Frequency	Show minor tuning thickness at 2 and 1 ms
Single Frequency	9 ms

CONCLUSION

This study demonstrated that source-wavelet frequency content plays a critical role in controlling the seismic expression, tuning behaviour, and resolution of pinch-out structures. Based on the synthetic wedge model, the comparison between a conventional 45 Hz Ricker wavelet and a broadband wavelet showed significant differences in waveform characteristics, amplitude responses, and the ability to resolve progressively thinning layers. The 45 Hz wavelet produced stronger tuning effects, where interference between reflections from closely spaced interfaces caused amplitude distortion and reduced the accuracy of apparent layer-thickness estimation. In contrast, the broadband wavelet provided a more compact seismic response with reduced interference effects, enabling clearer separation of thin interfaces and improved representation of the wedge termination.

The synthetic modelling results indicated that the 45 Hz wavelet generated a distinct tuning thickness at approximately 9 ms, whereas the broadband wavelet minimized tuning

effects and maintained better reflector separation at thinner layer conditions, with only minor tuning responses observed near 2 ms and 1 ms. These findings confirm that increasing frequency bandwidth improves seismic detectability by reducing the overlap of reflected wavelets and preserving more reliable amplitude and waveform information. The results also highlight that seismic amplitude anomalies in thin-bed environments should not be interpreted independently because they are strongly influenced by wavelet characteristics, bandwidth, impedance contrast, and layer thickness.

The integration of waveform analysis, interface amplitude evaluation, apparent-versus-true thickness comparison, and Rayleigh-based tuning assessment provided a comprehensive understanding of frequency-dependent seismic responses within a controlled pinch-out model. Although broadband wavelets demonstrated superior performance in resolving thin geological features, their application in real seismic data remains dependent on factors such as noise level, attenuation, acquisition quality, and processing methods. Therefore, careful evaluation of wavelet properties remains essential before interpreting thin reservoirs and stratigraphic terminations.

Overall, this research provides a synthetic reference for understanding how source-wavelet selection influences thin-bed and pinch-out interpretation. The findings emphasize that broadband frequency approaches can enhance seismic resolution and reduce tuning-related ambiguity compared with conventional single-frequency wavelets. This study contributes to improved seismic interpretation workflows by supporting more accurate wavelet selection, frequency assessment, and recognition of frequency-dependent effects during reservoir characterization and exploration activities.

REFERENCES

Alcalde, J., & Bond, C. E. (2022). Subjective uncertainty and biases: The impact on seismic data interpretation. In *Interpreting subsurface seismic data* (pp. 103–123). Elsevier.

An, Y., & Dong, R. (2023). Understanding the effect of different prior knowledge on CNN fault interpreter. *IEEE Access, 11*, 15058–15068.

Anna, K., Tomasz, M., Piotr, H., & Ryszard, H. (2026). Spectral decomposition of seismic data: Unlocking lithological insights into clastic sediments interpretation within fold-and-thrust settings of the northern Outer Carpathians, Poland. *Marine Geoscience and Energy Resources*, 207661.

Chang, Y.-C., Hsiung, K.-H., Kanamatsu, T., Nakanishi, R., Yamamoto, Y., & Uramoto, G.-I. (2026). A widespread meter-thick turbidite in the Southern Kuril Trench records the 13th-century megathrust earthquake. *Geoscience Letters, 13*(1), 29.

Chatterjee, S., Zhao, H., & Zhang, S. (2025). Seismic waveform-driven characterization using full frequency inversion (FFI): A case study in enhanced seismic reservoir characterization from the North-West Shelf, offshore Australia. In *Abu Dhabi International Petroleum Exhibition and Conference*. SPE.

Gochioco, L. M. (1991). Tuning effect and interference reflections from thin beds and coal seams. *Geophysics, 56*(8), 1288–1295. https://doi.org/10.1190/1.1443151

Gunderson, K. L., Zhang, Z., Payne, B., Cheng, S., Jiang, Z., & Wang, A. (2022). Machine learning applications to seismic structural interpretation: Philosophy, progress, pitfalls, and potential. *AAPG Bulletin, 106*(11), 2187–2202.

Hilterman, F. J. (2013). *Seismic reflection amplitude objective: (3).* Society of Exploration Geophysicists.

Khalid, P., Farid, A., Naseer, M. T., Yasin, Q., & Naseem, S. (2023). Seismic stratigraphy and attributes application for imaging a Lower Cretaceous deltaic system: Sukkur rift zone, Lower Indus Basin, Pakistan. *Marine and Petroleum Geology, 149*, 106030.

Meissner, R., & Meixner, E. (1969). Deformation of seismic wavelets by thin layers and layered boundaries. *Journal of Chemical Information and Modeling, 53*(9), 1689–1699.

Okaya, D. A. (1995). Spectral properties of the Earth's contribution to seismic resolution. *Geophysics, 60*(1), 241–251. https://doi.org/10.1190/1.1443752

Peploe, T. G. E. (2026). *Multi-disciplinary analyses of outcropping Late Cretaceous clinoform stratigraphy, Magallanes Basin, Chile* [Doctoral dissertation, University of Calgary].

Ren, M., Huang, X., Cui, X., Yang, R., Zhang, R., Liu, J., & Niu, C. (2026). Low-velocity mudstone identification using well logs and prestack seismic data based on principal component analysis and multilayer perceptron. *Journal of Applied Geophysics*, 106424.

Russell, B. (1988). The convolutional model. In *Introduction to seismic inversion methods*. Society of Exploration Geophysicists. https://doi.org/10.1190/1.9781560802303.ch2

Schwardt, M., Pilger, C., Gaebler, P., Hupe, P., & Ceranna, L. (2022). Natural and anthropogenic sources of seismic, hydroacoustic, and infrasonic waves: Waveforms and spectral characteristics (and their applicability for sensor calibration). *Surveys in Geophysics, 43*(5), 1265–1361.

Simm, R., & Bacon, M. (2014). *Seismic amplitude interpretation*. Cambridge University Press.

Veeken, P. C. H. (2007). *Seismic stratigraphy, basin analysis, and reservoir characterization*. Elsevier. https://doi.org/10.1016/S0950-1401(07)80025-5

Verma, S., Chopra, S., Ha, T., & Li, F. (2022). A review of some amplitude-based seismic geometric attributes and their applications. *Interpretation, 10*(1), B1–B12.

Widess, M. B. (1973). How thin is a thin bed? *Geophysics, 38*(6), 1176–1180. https://doi.org/10.1190/1.1440403

Yang, H., Cui, S., Pei, X., Fan, X., & Lei, J. (2023). Multiple earthquake-induced progressive failure of bedding slopes with a saturated weak layer: Shaking table model tests. *Soil Dynamics and Earthquake Engineering, 170*, 107906.

Ye, Y., Zhang, B., Niu, C., Qi, J., & Zhou, H. (2019). The thickness imaging of channels using multiple-frequency components analysis. *Interpretation, 7*(1), B1–B8. https://doi.org/10.1190/INT-2018-0064.1

Zhang, F.-Y., Tang, J.-Z., Wu, H.-L., Liu, J., Zhou, J., Zhao, S.-J., Huang, F.-M., Zhang, J., Wang, H., & Li, J.-L. (2026). Geological fault identification via multi-knowledge causally embedding graph representation applied in underground gas storage. *Petroleum Science* [Preprint].